



ORIGINAL ARTICLE

Generation of combined hepatocellular-cholangiocarcinoma through transdifferentiation and dedifferentiation in p53-knockout mice

Yang Liu^{1,2} | Bing Xin¹ | Masahiro Yamamoto¹ | Masanori Goto¹ | Takako Ooshio¹ | Yuki Kamikokura¹ | Hiroki Tanaka¹ | Lingtong Meng¹ | Yoko Okada¹ | Yusuke Mizukami³  | Yuji Nishikawa¹ 

¹Department of Pathology, Division of Tumor Pathology, Asahikawa Medical University, Asahikawa, Japan

²Department of Pathology, the First Affiliated Hospital and College of Basic Medical Sciences of China Medical University, Shenyang, China

³Department of Medicine, Cancer Genomics and Precision Medicine, Asahikawa Medical University, Asahikawa, Japan

Correspondence

Yuji Nishikawa, Division of Tumor Pathology, Department of Pathology, Asahikawa Medical University, Higashi 2-1-1-1, Midorigaoka, Asahikawa, Hokkaido 078-8510, Japan.
Email: nishikwa@asahikawa-med.ac.jp

Funding information

This study was supported by grants from the Japan Society for the Promotion of Science (#15K15107 and #19H03448 to YN) and the Akiyama Life Science Foundation (to YN).

Abstract

The two principal histological types of primary liver cancers, hepatocellular carcinoma (HCC) and cholangiocarcinoma, can coexist within a tumor, comprising combined hepatocellular-cholangiocarcinoma (cHCC-CCA). Although the possible involvement of liver stem/progenitor cells has been proposed for the pathogenesis of cHCC-CCA, the cells might originate from transformed hepatocytes that undergo ductular transdifferentiation or dedifferentiation. We previously demonstrated that concomitant introduction of mutant HRAS^{V12} (HRAS) and Myc into mouse hepatocytes induced dedifferentiated tumors that expressed fetal/neonatal liver genes and proteins. Here, we examine whether the phenotype of HRAS- or HRAS/Myc-induced tumors might be affected by the disruption of the *Trp53* gene, which has been shown to induce biliary differentiation in mouse liver tumors. Hepatocyte-derived liver tumors were induced in heterozygous and homozygous p53-knockout (KO) mice by hydrodynamic tail vein injection of HRAS- or Myc-containing transposon cassette plasmids, which were modified by deleting loxP sites, with a transposase-expressing plasmid. The HRAS-induced and HRAS/Myc-induced tumors in the wild-type mice demonstrated histological features of HCC, whereas the phenotype of the tumors generated in the p53-KO mice was consistent with cHCC-CCA. The expression of fetal/neonatal liver proteins, including delta-like 1, was detected in the HRAS/Myc-induced but not in the HRAS-induced cHCC-CCA tissues. The dedifferentiation in the HRAS/Myc-induced tumors was more marked in the homozygous p53-KO mice than in the heterozygous p53-KO mice and was associated with activation of Myc and YAP and suppression of ERK phosphorylation. Our results suggest that the loss of p53 promotes ductular differentiation of hepatocyte-derived tumor cells through either transdifferentiation or Myc-mediated dedifferentiation.

This is an open access article under the terms of the Creative Commons Attribution-NonCommercial-NoDerivs License, which permits use and distribution in any medium, provided the original work is properly cited, the use is non-commercial and no modifications or adaptations are made.

© 2021 The Authors. *Cancer Science* published by John Wiley & Sons Australia, Ltd on behalf of Japanese Cancer Association.

KEYWORDS

animal model for carcinogenesis, cell differentiation, characteristics of cancer cells, experimental animal models and genetically engineered animals, gene-manipulated animal models, oncogenes and tumor-suppressor genes, p53-related genes

1 | INTRODUCTION

Understanding the pathogenesis of primary liver cancer is indispensable for combatting this intractable malignancy. Although hepatocellular carcinoma (HCC) and cholangiocarcinoma (CCA) are the principal histological types of liver cancer, there are a variety of tumor phenotypes, including combined hepatocellular-cholangiocarcinoma (cHCC-CAA), in which HCC and CCA cells coexist within the same tumor.¹ The pathogenesis and cellular origins of cHCC-CAA have been a subject of debate. Some researchers suppose that cHCC-CAA originate from putative hepatic stem/progenitor cells,² which have been thought to reside in the adult liver and possess the capacity for both hepatocellular and biliary differentiation.³ However, there has been no solid evidence to support this notion. Furthermore, based on accumulated evidence, the initial hepatic stem/progenitor hypothesis has been reconsidered.⁴

During liver organogenesis, hepatoblasts, which emerge at the hepatic diverticulum, proliferate and differentiate into liver epithelial cells, including hepatocytes and bile duct/ductular cells. Hepatocytes and intrahepatic bile ducts/ductules are derived from hepatoblasts that express albumin, while extrahepatic bile duct cells originate from less differentiated hepatoblasts prior to the acquisition of albumin expression.^{5,6} Activation of the Notch pathway has been shown to be crucial in bile duct differentiation of hepatoblasts.⁷ Although it was presumed that the phenotype of terminally differentiated hepatocytes is fixed,⁸ experimental studies using rodent hepatocytes have demonstrated that these cells retain phenotypic plasticity, especially transdifferentiation into bile duct/ductular cells *in vitro* and *in vivo*.^{6,9-11}

Using transposon-mediated gene integration into the genome of mouse hepatocytes and by combining oncogene-harboring transposons with hydrodynamic gene transfer, mature hepatocytes have been shown to generate a wide spectrum of liver tumors.^{12,13} The combinations of NRAS or HRAS with activated (myristoylated) AKT induce HCC with ductular structures, similar to the phenotype of cHCC-CAA.^{14,15} It has also been shown that mature hepatocytes can generate CCA when they are transformed by the activated AKT and Notch intracellular domain (NICD), by activated PIK3CA and Yes-associated protein (YAP), or by activated AKT and YAP.¹⁶⁻¹⁸ A genome-wide transcriptional analysis of human primary liver tumors has also suggested the possibility that there is a continuum of poorly differentiated HCC, cHCC-CCA, and CCA.¹⁹

It is not clear whether the generation of cHCC-CCA is due to partial transdifferentiation toward bile ducts/ductules or via dedifferentiation toward hepatoblasts. We have demonstrated that, whereas transposon-mediated HRAS introduction in hepatocytes induces typical HCC, concomitant introduction of HRAS and Myc

induces dedifferentiated liver tumors with hepatoblastic gene and protein expression and no biliary differentiation.²⁰ Furthermore, we found that the combination of activated YAP and Myc induces cHCC-CCA with the expression of hepatoblastic markers and that the dedifferentiated features are abolished by the superimposed introduction of activated AKT.¹⁸ These findings suggest that mature hepatocytes can be dedifferentiated to acquire a hepatoblastic phenotype upon Myc activation in cooperation with other oncogenes to generate cHCC-CCA.

In human HCC, the function of the p53 protein is frequently inhibited due to mutation or loss of the *TP53* gene or nonmutated p53-inactivating mechanisms.²¹ It has been shown that the genomic profile of cHCC-CCA is more similar to that of HCC than that of CCA and that *TP53* is the most frequently mutated gene in cHCC-CCA.²²⁻²⁴ Upon a liver-specific conditional knockout of p53, in which the deletion of *Trp53* is evident in all intrahepatic epithelial cells (hepatocytes, bile duct/ductular cells, and possibly liver stem/progenitor cells), it has been reported that liver tumors with bidirectional (hepatocytic and bile ductular) differentiation are generated, suggesting that the loss of p53 might affect the phenotype of primary liver cancer.²⁵ Furthermore, as p53 and Myc have been shown to negatively regulate each other,²⁶ dysfunctional p53 may enhance Myc-mediated dedifferentiation. However, the roles of p53 in the phenotypic determination of hepatocyte-derived tumors have not yet been elucidated.

In this study, we examined whether the tumor phenotypes of HRAS- or HRAS/Myc-induced tumors are affected by hepatocyte-specific p53 knockout. We found that the loss of p53 drives biliary differentiation in these tumors through transdifferentiation, as well as dedifferentiation, which is associated with Myc and YAP activation and the suppression of ERK phosphorylation. Our results provide mechanistic insights into the pathogenesis of cHCC-CAA.

2 | MATERIALS AND METHODS

2.1 | Animal experiments

C57BL/6J mice were purchased from Charles River Laboratories Japan. Mice containing a floxed *Trp53* gene were purchased from Jackson Laboratories. At the end of the animal experiments, the mice were euthanized under deep anesthesia, and the livers were removed for further examination. The protocols used for animal experimentation were approved by the Animal Research Committee, Asahikawa Medical University, and all animal experiments adhered to the criteria outlined in the Guide for the Care and Use of Laboratory Animals prepared by the National Academy of Sciences (8th Ed., 2011).

2.2 | Generation of hepatocyte-specific p53-KO mice

To generate heterozygous or homozygous hepatocyte-specific p53-KO mice, p53^{fl/+} or p53^{fl/fl} mice were injected via the lateral tail vein with 1×10^{12} copies of adeno-associated virus serotype 8 (AAV8) expressing Cre recombinase under the control of a hepatocyte-specific thyroxine-binding globulin (TBG) promoter (AAV8-TBG-Cre). AAV8-TBG-Cre was prepared by the triple-transfection method with pENN-AAV-TBG-PI-Cre-rBG, pBS-E2A-VA-E4, and p5E18-VD2/8 plasmids into 293T cells.¹⁸

2.3 | Plasmids

A Sleeping Beauty (SB) 13 transposase-expressing vector (pT2/C-Luc/PGK-SB13, Addgene plasmid #20207) and a myrAKT-HA-expressing transposon cassette vector (pT3-EF1 α -myrAKT-HA, Addgene plasmid #31789) was purchased from Addgene. cDNA fragments of FLAG-HRASV12 and enhanced green fluorescent protein (EGFP) were amplified from pTomo-Ras (Addgene plasmid #26292) and pCMV-EGFP (Takara Bio), respectively. A full-length Myc fragment was amplified from the cDNA of diethylnitrosamine-induced mouse liver tumors.¹⁵ The two loxP sites in the original pT3-EF1 α -myrAKT-HA plasmid were removed with a GENEART site-directed mutagenesis system (Thermo Fisher Scientific).¹⁸ Then, the cDNA fragments were cloned into the modified pT3-EF1 α plasmid after removing the myrAKT-HA fragment with a Gateway system (Thermo Fisher Scientific). All plasmids were amplified and purified using an EndoFree Plasmid Maxi kit (Qiagen).

2.4 | Transposon-mediated introduction of oncogenes into mouse hepatocytes in vivo

The combination of the SB transposon system and hydrodynamic tail vein injection (HTVi) was used to introduce genes into hepatocytes in vivo. The transposon cassette plasmids (pT3-EF1 α -HRASV12 + pT3-EF1 α -EGFP, pT3-EF1 α -HRASV12 + pT3-EF1 α -Myc) were coinjected with an SB13 transposase-expression plasmid into male wild-type, heterozygous p53-KO or homozygous p53-KO mice (from 8 to 12 weeks old). For HTVi, plasmids were dissolved in 2.5 mL of Ringer solution and rapidly injected, within 8 seconds, into the lateral tail veins of the mice. The total amount of plasmid DNA was 25 μ g for mixtures of three different plasmids (including the transposase-expressing vector). Equimolar amounts of each transposon cassette plasmid containing the genes were mixed, and the molar ratio of the transposase-expressing vector to each transposon cassette plasmid was 1:2.

To estimate the copy numbers of the integrated Myc-harboring plasmids per genome, we extracted genomic DNA from tumor samples with a DNeasy Blood & Tissue kit (Qiagen) and performed quantitative real-time polymerase chain reaction (qPCR) analyses using

FastStart Universal SYBR Green Master Mix (Roche Diagnostics). The amounts of genomic DNA from the tumor samples were normalized by estimation of the copy numbers of the endogenous *Notch2* gene. The quantification cycle (Cq) values obtained in each tumor were interpolated on standard curves representing known copy numbers of Myc-containing plasmids vs their corresponding Cq values. The sequences of the specific primers are listed in Supporting Table 1.

2.5 | Microscopic examination and immunohistochemistry

The livers were fixed in phosphate-buffered 4% paraformaldehyde for 24 hours at 4°C, and paraffin sections were prepared. Immunohistochemical analysis was performed using an EnVision/HRP system (DAKO) on deparaffinized sections treated with target retrieval solution (DAKO). The following antibodies were used: anti-p53 (Novocastra, Leica Microsystems), anti-cytokeratin 19 (CK19) (provided by Dr Atsushi Miyajima, Institute for Quantitative Biosciences, The University of Tokyo), anti-Hes1 (Cell Signaling Technology), anti-YAP (kindly provided by Dr Hiroshi Nishina, Department of Developmental and Regenerative Biology, Medical Research Institute, Tokyo Medical and Dental University), anti- α -fetoprotein (AFP) (Proteintech), anti-insulin-like growth factor 2 (IGF2) (Abcam), anti-delta-like 1 protein (DLK1) (Medical & Biological Laboratories), anti-5-hydroxymethylcytosine (5hmC; Active Motif), anti-Myc (Abcam), anti-phosphorylated ERK (Cell Signaling Technology), and anti-Ki-67 (Nichirei). The chromogen 3,3'-diaminobenzidine tetrahydrochloride was used to detect the signal (Vector Laboratories), and the sections were counterstained with hematoxylin.

2.6 | Reverse transcription quantitative polymerase chain reaction (RT-qPCR)

Total RNA was extracted and subjected to RT-qPCR analyses. RT-qPCR was performed using the $\Delta\Delta$ Ct method with FastStart Universal SYBR Green Master Mix (Roche Diagnostics). Each reaction was conducted in duplicate, and the mRNA levels were normalized to the expression of the hypoxanthine phosphoribosyl-transferase gene (*Hprt*). The primers used in the RT-qPCR experiments are listed in Supporting Table 1.

2.7 | Statistical analyses

All data are presented as the means \pm SEM. Statistical analyses were performed using the Mantel-Cox test, Kruskal-Wallis test, one-way analysis of variance (ANOVA) with Tukey's post hoc test, Mann-Whitney *U*-test, or unpaired two-tailed *t*-test. Statistical analyses were performed using GraphPad Prism (version 7.00, GraphPad Software).

3 | RESULTS

3.1 | Facilitation of HRAS/Myc-induced, but not HRAS-induced, hepatocarcinogenesis through the disruption of p53

The introduction of HRAS alone induced liver tumors in both wild-type and homozygous p53-KO mice after approximately 3 months (Figure 1A). Although the tumors in the p53-KO mice appeared more diffuse and extensive, the courses of tumorigenesis were comparable between the wild-type and p53-KO mice (Figure 1A). In contrast, the cointroduction of HRAS and Myc induced multiple discrete tumors, and tumorigenesis was significantly facilitated by p53 KO, in particular, by homozygous KO (Figure 1B).

3.2 | cHCC-CCA-like histology of liver tumors induced by HRAS or HRAS/Myc in the p53-KO mice

The histological features of the liver tumors induced only by HRAS in the wild-type mice were typical of HCC, but in some of the HRAS-induced tumors in the p53-KO mice, a component containing distinct ductular structures formed by atypical cells with desmoplastic reaction were intermingled with HCC, rendering the histological type compatible with cHCC-CCA (Figure 2A). Compared with HRAS/Myc-induced tumors generated in the wild-type mice that demonstrated the histology of HCC, those generated in the p53-KO mice contained histological features of both HCC and CCA within the same lesions in most of the well-developed tumors (Figure 2A). HRAS/Myc-induced tumors in the homozygous p53-KO mice appeared to be less differentiated, with sheet-like proliferation of atypical tumor cells containing

prominent nucleoli and inconspicuous ductular structures, than the HRAS-induced tumors in the homozygous p53-KO mice or HRAS/Myc-induced tumors in the heterozygous p53-KO mice (Figure 2A). In both HRAS-induced and HRAS/Myc-induced tumors in the wild-type mice, p53 protein was detected in the nuclei of tumor cells (Figure 2B). However, as expected, the tumors generated in homozygous p53-KO mice were negative for p53, while those generated in heterozygous p53-KO demonstrated weak immunoreactivity (Figure 2B).

The immunohistochemical analyses revealed that the tumor component with ductular structures was positive for CK19, a marker for bile ducts/ductules (Figure 3A). The expression of *Krt19* mRNA was detected in the HRAS-induced and HRAS/Myc-induced tumors in the p53-KO mice (Figure 3B). The mRNA expression of *Sox9*, another marker for bile ducts/ductules, as well as putative liver stem/progenitor cells, was detected in the HRAS-induced and HRAS/Myc-induced tumors in the wild-type mice, which did not contain a CCA component, but the expression was suppressed in the HRAS/Myc-induced tumors in the homozygous p53-KO mice (Figure 3B). As the Notch pathway is known to be involved in bile duct differentiation, we examined the expression of *Hes1*, an effector of its pathway. Nuclear *Hes1* expression was detected in tumor cells in the areas of ductular differentiation, although its weak expression was also seen in both HRAS-induced and HRAS/Myc-induced tumors in the wild-type mice (Figure 3C). We also examined the expression of YAP, which interacts with the Notch pathway,²⁷ and found that nuclear accumulation of YAP was particularly prominent in the HRAS/Myc-induced tumors with p53 disruption (Figure 3C). Whereas *Hnf4a* mRNA expression was detected at various levels in all the tumors examined, its expression in the HRAS/Myc-induced tumors in the wild-type mice was significantly higher than that in the normal liver tissues

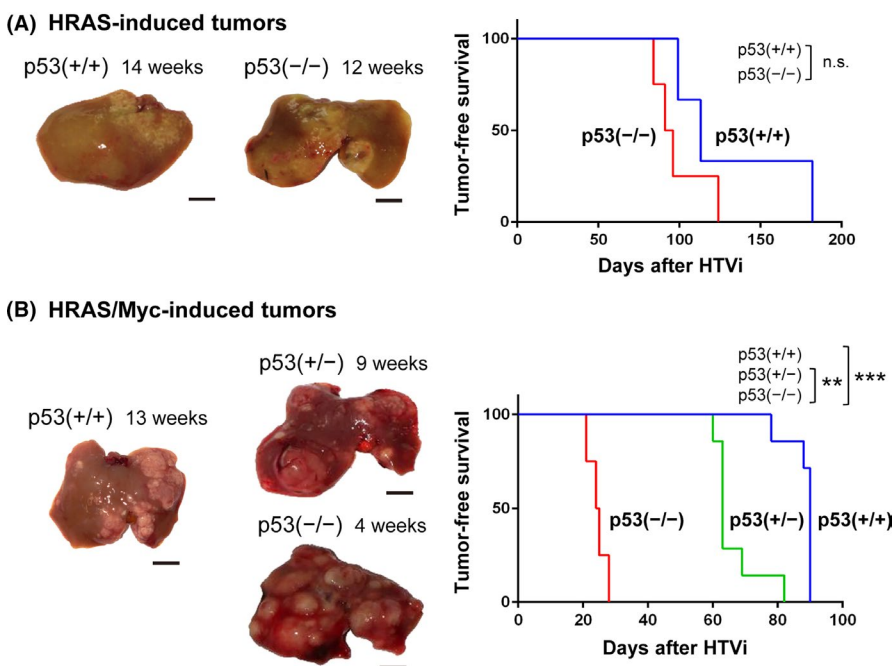


FIGURE 1 Effects of p53 disruption on hepatocarcinogenesis induced by the transposon-mediated integration of HRAS or HRAS/Myc. Gross appearance of the liver tumors and tumor-free survival of the mice after the introduction of the oncogene(s). A, HRAS-induced tumors. B, HRAS/Myc-induced tumors. p53(+/+), wild type; p53(+/-), heterozygous p53-knockout (KO); and p53(-/-), homozygous p53-KO. n = 3 for HRAS (+/+), n = 4 for HRAS (-/-); n = 7 for HRAS/Myc (+/+), HRAS/Myc (+/-); n = 5 for HRAS/Myc (-/-). Statistical analysis: Mantel-Cox test. ***P* < .01 and ****P* < .001. n.s., not significant. Scale bars = 5 mm

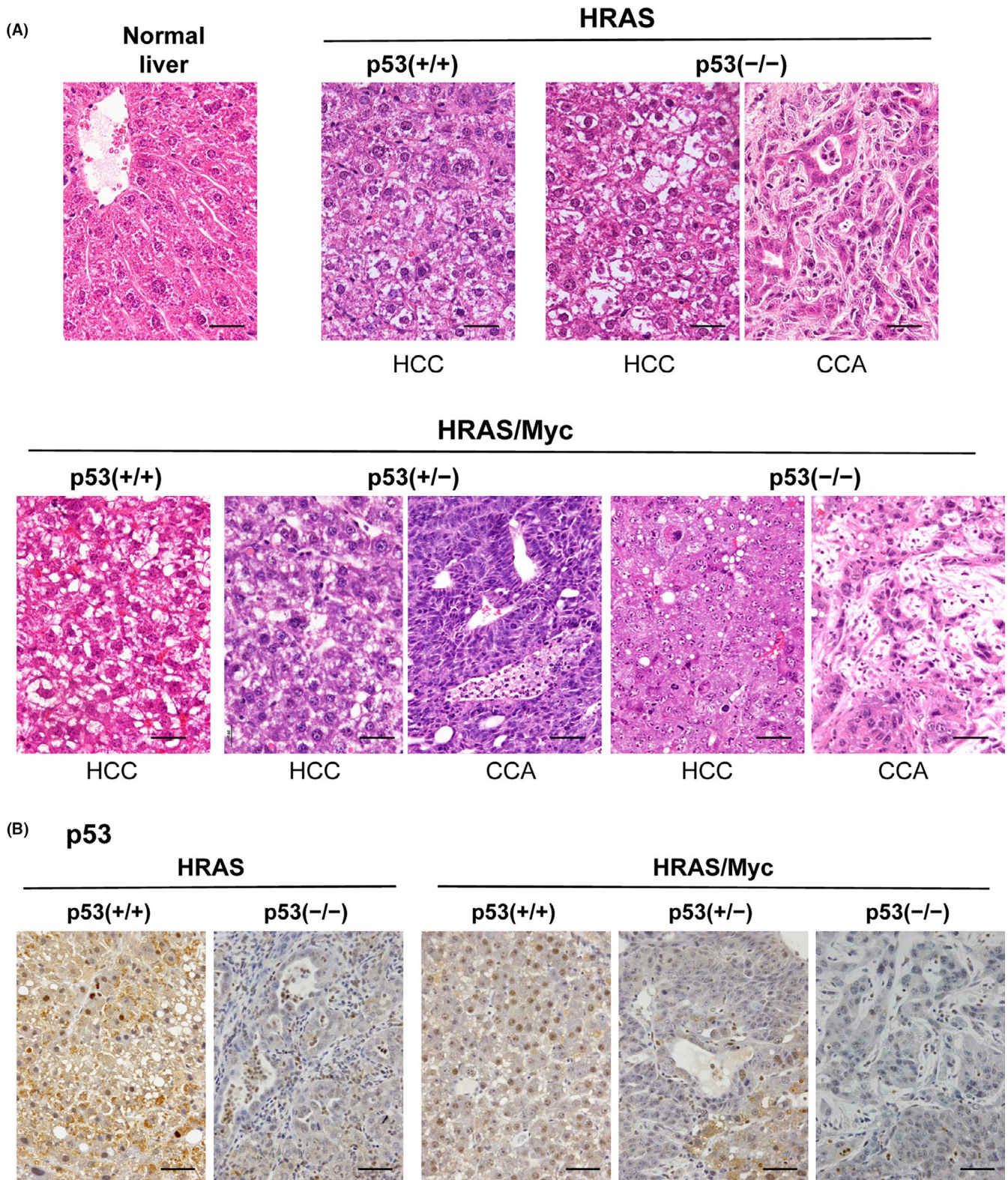
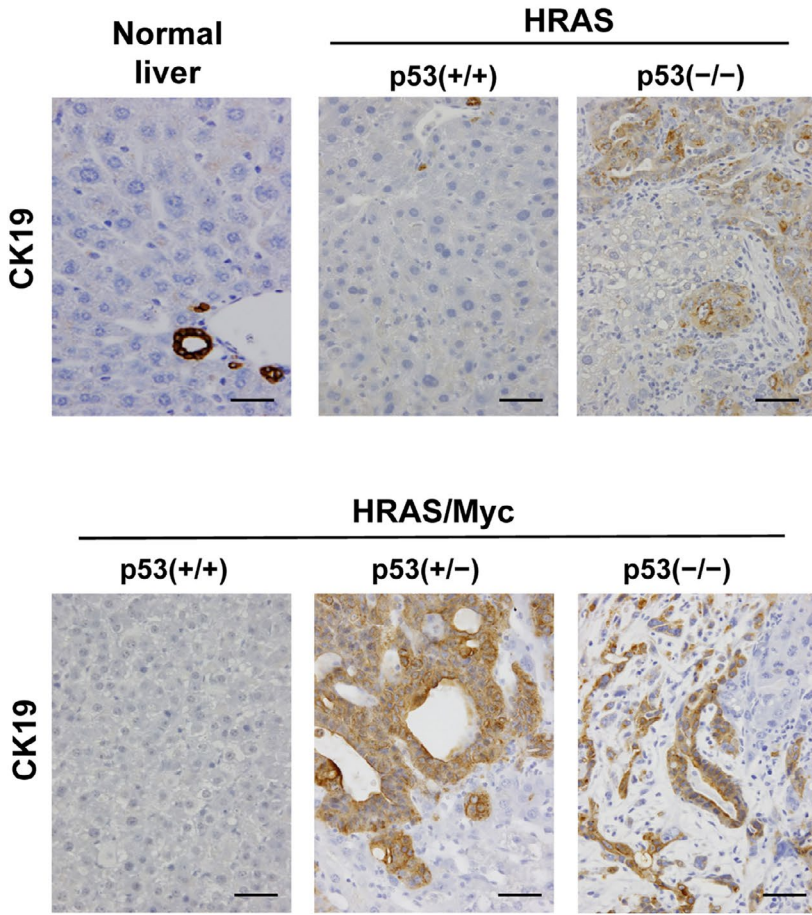


FIGURE 2 Histological features of liver tumors induced by HRAS or HRAS/Myc in wild-type and p53-KO mice. A, Hematoxylin and eosin (HE) staining. B, Immunohistochemistry for p53. p53(+⁺), wild type; p53(+/-), heterozygous p53-knockout (KO); and p53(-/-), homozygous p53 KO. Scale bar = 40 μ m

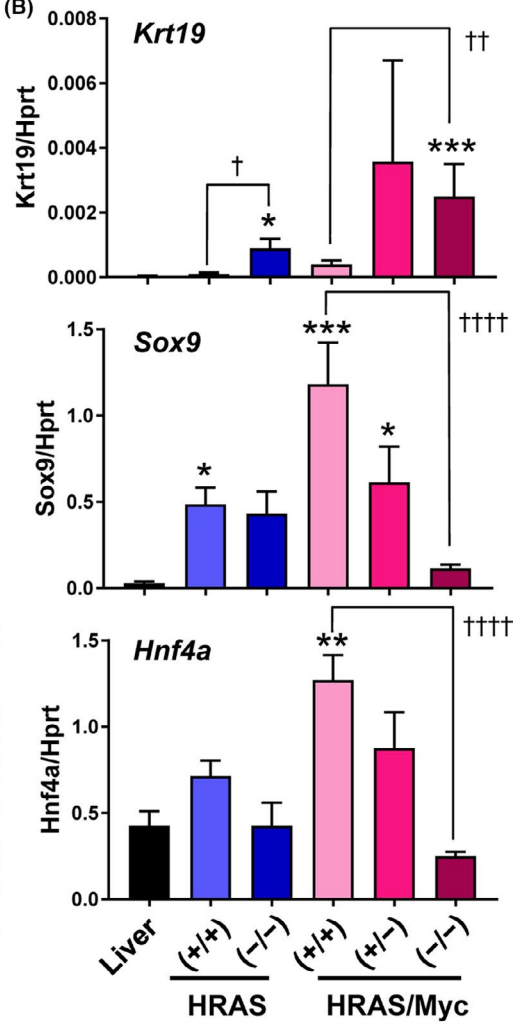
(Figure 3B). However, the expression of *Hnf4a* mRNA in the tumors in the homozygous p53-KO mice was decreased compared with that in the wild-type mice (Figure 3B). The suppression of

Sox9 and *Hnf4a* gene expression in the HRAS/Myc-induced tumors in the homozygous p53-KO mice might reflect a dedifferentiated tumor state.

(A)



(B)



(C)

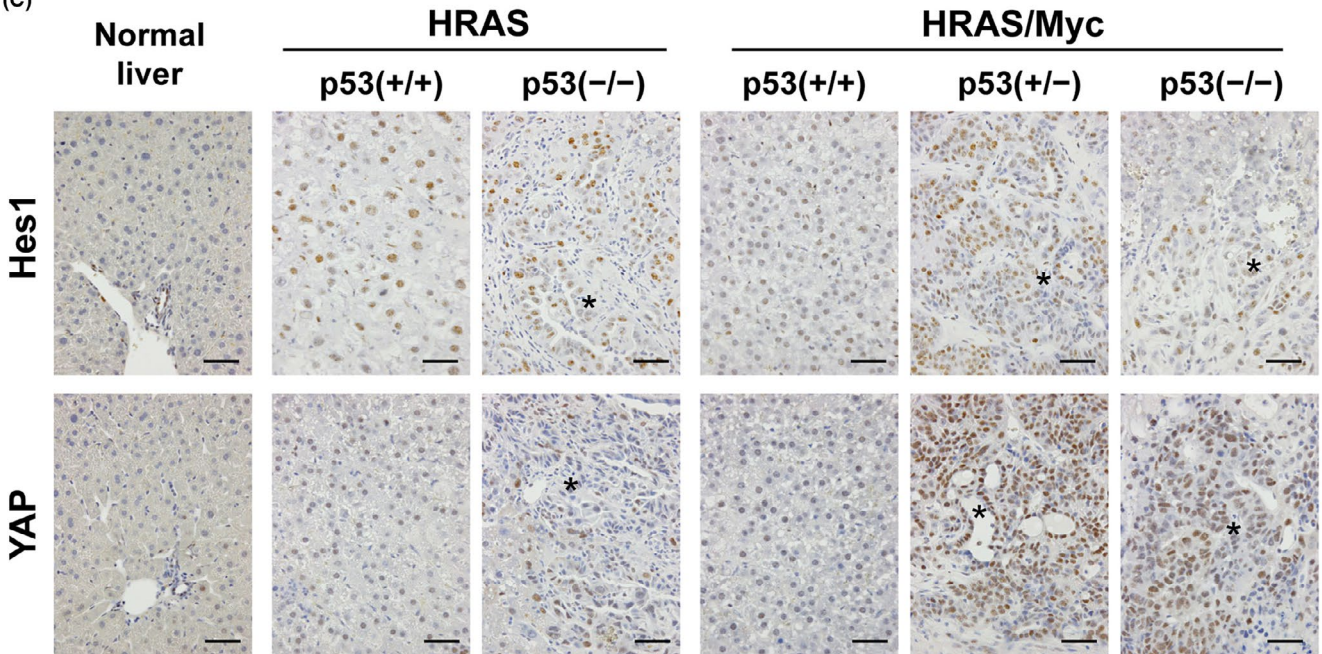


FIGURE 3 Effects of p53 disruption on the expression of biliary and hepatocytic markers in tumors induced by HRAS or HRAS/Myc. A, Immunohistochemistry for cytokeratin 19 (CK 19). p53(+/+), wild type; p53(+/-), heterozygous p53-KO; and p53(-/-), homozygous p53-KO. Scale bar = 40 μ m. B, Quantitative RT-PCR analyses of the expression of bile duct-specific (*Krt19*, *Sox9*) and hepatocyte-specific (*Hnf4a*) genes. $n = 4$ for normal liver, HRAS (+/+), and HRAS (-/-); $n = 6$ for HRAS/Myc (+/+), HRAS/Myc (+/-), and HRAS/Myc (-/-). Statistical analyses: Kruskal-Wallis test (*Krt19*, *Sox9*) or one-way analysis of variance (ANOVA) with Tukey's post hoc test (*Hnf4a*), * $P < .05$, ** $P < .01$ and *** $P < .001$ (vs normal liver); Mann-Whitney U test (*Krt19*, *Sox9*) or unpaired two-tailed t -test (*Hnf4a*), † $P < .05$, †† $P < .01$, and †††† $P < .0001$. C, Immunohistochemistry for Hes1 and YAP. Asterisks denote the areas of biliary differentiation in tumors. Scale bar = 40 μ m

3.3 | The expression of fetal/neonatal liver genes in HRAS/Myc-induced tumors and their augmentation by p53 KO

We then examined whether HRAS- and HRAS/Myc-induced tumors underwent dedifferentiation by performing an immunohistochemical analysis of the AFP, IGF2, and DLK1 levels, which are expressed in the liver during the fetal/neonatal period. The HRAS-induced tumors did not express these proteins in either the wild-type mice or homozygous p53-KO mice (Figure 4A). In HRAS/Myc-induced tumors in the wild-type mice, the AFP and IGF2 proteins were weakly expressed, but the expression of the DLK1 protein was not detected (Figure 4A). The expression of the AFP and IGF2 proteins in the HRAS/Myc-induced tumors was increased in both the heterozygous and homozygous p53-KO mice (Figure 4A). DLK1 protein was detected in the HRAS/Myc-induced tumors in the p53-KO mice; the expression levels in the homozygous p53-KO mice were higher than those in the heterozygous p53-KO mice (Figure 4A). Compatible with the immunohistochemical data, the mRNA expression of *Afp*, *Igf2*, *Dlk1*, and *H19* noncoding RNA was not detected in the HRAS-induced tumors in either the wild-type mice or homozygous p53-KO mice (Figure 4B). The mRNA expression of *H19* and *Igf2* was detected in the HRAS/Myc-induced tumors in both the wild-type mice and p53-KO mice (Figure 4B). Although the expression of *Afp* was detected at low levels in the HRAS/Myc-induced tumors in the wild-type mice and heterozygous p53-KO mice, its expression was significantly higher in the tumors in the homozygous p53-KO mice (Figure 4B). *Dlk1* mRNA was not expressed in the HRAS/Myc-induced tumors in the wild-type mice, but it was induced in the tumors in the p53-KO mice and was more robustly induced in the homozygous p53-KO mice (Figure 4B).

3.4 | Changes in the expression of the genes involved in DNA methylation and demethylation and 5hmC levels in the HRAS- and HRAS/Myc-induced tumors

As we previously found that epigenetic alterations are associated with the dedifferentiation of liver tumors,²⁰ the mRNA expression of enzymes involved in DNA methylation and demethylation was examined. There were significant increases in *Dnmt1*, which encodes a maintenance DNA methyltransferase, in the HRAS-induced and HRAS/Myc-induced tumors in the p53-KO mice (Figure 5A). The mRNA expression of *Dnmt3a* and *Dnmt3b*, which encode de novo

DNA methyltransferases, was increased in the HRAS/Myc-induced tumors in the wild-type and heterozygous p53-KO mice, but it was suppressed in the homozygous p53-KO mice (Figure 5A). The mRNA expression of *Tet1* coding a DNA demethylase was increased in the HRAS-induced tumors in p53-KO mice (Figure 5A). Although there was considerable variability among individual tumor samples, most HRAS/Myc-induced tumors in the wild-type and p53-KO mice expressed *Tet1* mRNA (Figure 5A). Immunohistochemistry for 5hmC, an intermediate that is generated during active demethylation, revealed that the immunoreactivity was stronger in the nuclei of HRAS- and HRAS/Myc-induced tumors in p53-KO mice, with a tendency to be more conspicuous in the latter (Figure 5B).

3.5 | Myc activation, ERK dephosphorylation, and increased proliferative activity of the HRAS/Myc-induced tumors in the p53-KO mice

We then examined the effects of p53 disruption on Myc expression and the phosphorylation of ERK, as well as on the proliferative activity of the tumors. Myc protein was not detectable in the HRAS-induced tumors in the wild-type mice, but weak expression was noted in the tumors generated in the homozygous p53-KO mice (Figure 6A). In the HRAS-induced tumors in the wild-type mice and homozygous p53-KO mice, ERK was extensively phosphorylated (Figure 6A). The proliferative activity of the HRAS-induced tumors, which was estimated by Ki-67 immunohistochemistry, was not affected by p53 KO (Figure 6A). In the HRAS/Myc-induced tumors in the wild-type mice, the expression of Myc protein was very weak, but ERK was markedly phosphorylated (Figure 6A). However, in the p53-KO mice, the expression of the Myc protein was significantly augmented, whereas ERK phosphorylation was suppressed, especially in the homozygous p53-KO mice, in which nuclear staining of phosphorylated ERK was negligible (Figure 6A). In the HRAS/Myc-induced tumors in the homozygous p53-KO mice, Ki-67 labeling was markedly increased (Figure 6A).

There was a slight increase in the expression of endogenous Myc mRNA in the HRAS-induced tumors in the homozygous p53-KO mice (Figure 6B). The increase in Myc mRNA was accompanied by a significant increase of *Aurka* gene expression (Supplementary Figure 1), which is in accordance with the previous report showing that the interaction between Myc and aurora kinase A is critically important in Trp53-deficient, NRAS-driven HCC.²⁸ Compatible with our findings that the expression of Myc protein in the HRAS/Myc-induced tumors was low in the wild-type mice but increased in the

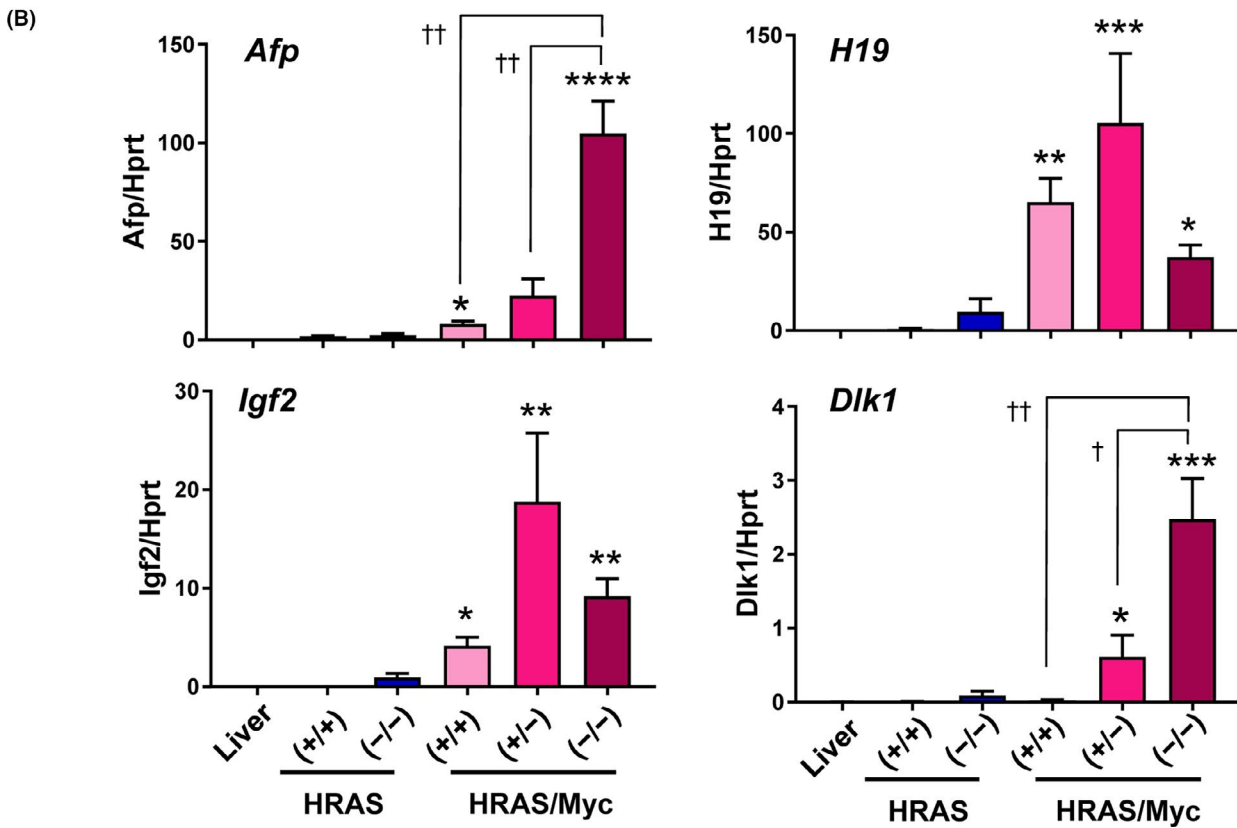
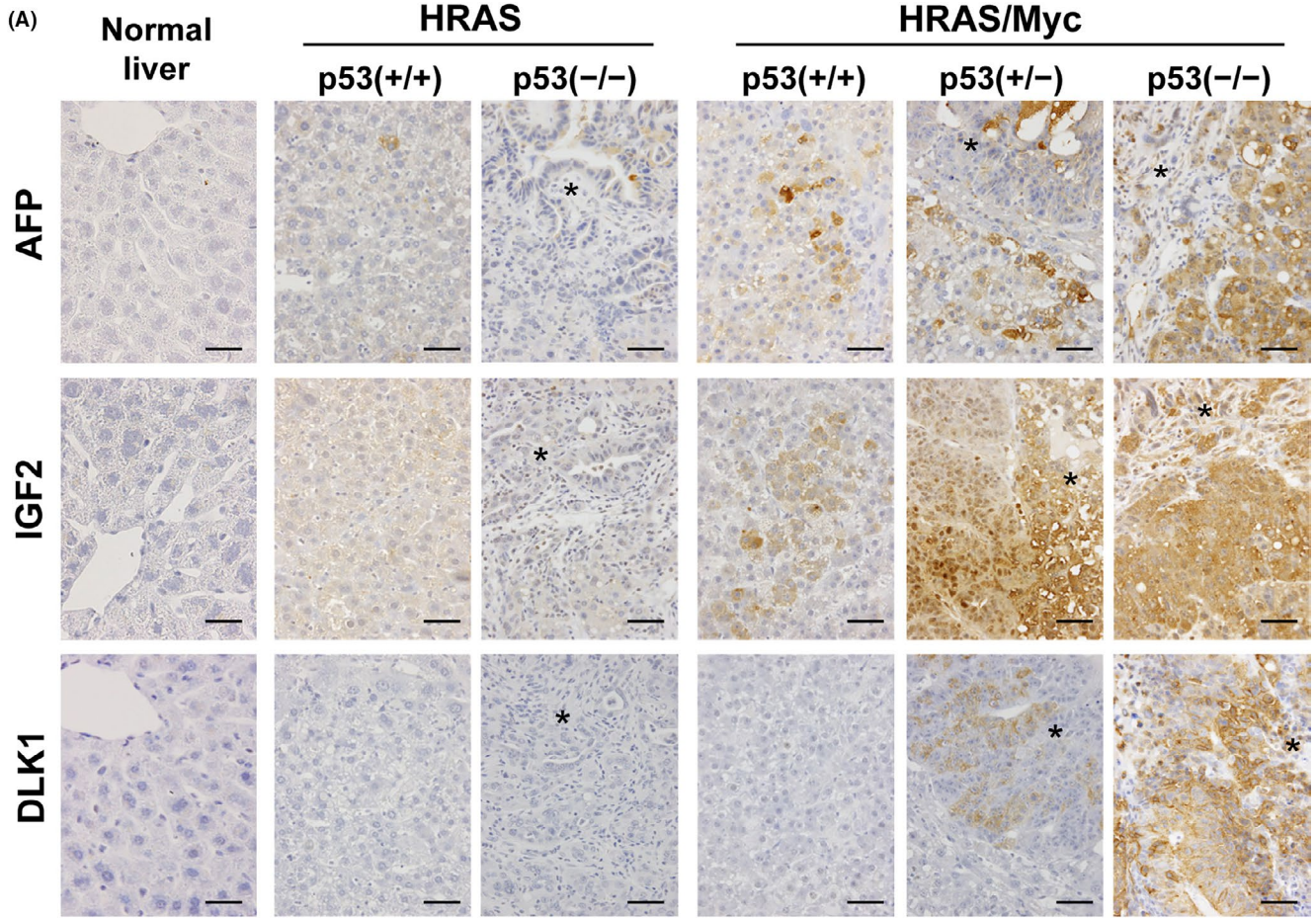


FIGURE 4 Effects of p53 disruption on the expression of hepatoblastic proteins and the mRNA expression of the genes activated in hepatoblasts in tumors induced by HRAS or HRAS/Myc. A, Immunohistochemistry for α -fetoprotein (AFP), insulin-like growth factor 2 (IGF2), and delta-like 1 (DLK1). p53(+/+), wild type; p53(+/-), heterozygous p53-KO; and p53(-/-), homozygous p53-KO. Asterisks denote the areas of biliary differentiation in tumors. Scale bar = 40 μ m. B, Quantitative RT-PCR analyses of the expression of *Afp*, *H19*, *Igf2*, and *Dlk1*. p53(+/+), wild type; p53(+/-), heterozygous p53-KO; and p53(-/-), homozygous p53-KO. n = 4 for normal liver, HRAS (+/+), and HRAS (-/-); n = 6 for HRAS/Myc (+/+), HRAS/Myc (+/-), and HRAS/Myc (-/-). Statistical analyses: Kruskal-Wallis test, * $P < .05$, ** $P < .01$, *** $P < .001$, and **** $P < .0001$ (vs normal liver); Mann-Whitney U test, † $P < .05$ and †† $P < .01$

p53-KO mice, the mRNA expression of exogenous *Myc* was low in the tumors in the wild-type mice but was increased in the tumors in the p53-KO mice (Figure 6C), which was not accompanied by significant increase in *Aurka* mRNA expression (Supplementary Figure 1). The mRNA expression of endogenous *Myc* was not affected by the introduction of exogenous *Myc* (Figure 6B). There was an increase in the copy numbers of the integrated *Myc*-harboring plasmids into the genome in the tumors in the p53-KO mice (Figure 6D), suggesting that p53 disruption permits the integration of more copies of the *Myc* gene and leads to its higher expression levels.

4 | DISCUSSION

In the present study, we demonstrated that disruption of the *Trp53* gene confers biliary differentiation to mouse liver tumors induced by the hepatocyte-specific introduction of either HRAS or HRAS and *Myc*. Hepatoblastic gene/protein expression was not associated with the HRAS-induced tumors in the homozygous p53-KO mice, suggesting that biliary differentiation is the result of the transdifferentiation of hepatocytes transformed by HRAS. The exhibition of similar biliary differentiation has been reported during the development of advanced HCC in humans.²⁹ In contrast, the HRAS/*Myc*-induced tumors in the heterozygous and homozygous p53-KO mice demonstrated marked expression of hepatoblastic markers, suggesting that biliary differentiation is associated with dedifferentiation. These results are compatible with previous data showing that the conditional depletion of p53 in the liver epithelial system induces liver tumors with biliary differentiation.²⁵ Our results clearly demonstrate that hepatocytes can generate cHCC-CCA when the function of p53 is disrupted through transdifferentiation or dedifferentiation.

As *Myc* is well known to be crucial in cellular reprogramming,³⁰ its activation in mouse hepatocytes has been demonstrated to induce the dedifferentiation tumors composed of hepatoblast-like tumor cells.³¹ We also reported that liver tumors induced by the combination of mutant HRAS or mutant YAP with *Myc* demonstrated dedifferentiated features with the expression of hepatoblastic markers, as well as mRNA expression of stem cell markers, such as *Nanog* and *Sox2*.^{18,20} In the present study, the dedifferentiation of HRAS/*Myc*-induced tumors was dependent on the levels of *Myc* activation, which was augmented in the p53-KO mice. *Myc* has been shown to be suppressed by p53 through several different mechanisms, which include not only direct transcriptional repression but also the induction of miR-145 and the lncRNA MILIP by p53.³²⁻³⁵ On the other hand, *Myc* induces the mRNA expression of the alternative reading

frame of p16^{INK} (ARF), which in turn activates p53.³⁶ *Myc* has been demonstrated to confer a cancer stem cell-like phenotype to human HCC cell lines when the function of p53 is disrupted.³⁷ Our study also demonstrated increases in nuclear YAP in tumors induced in p53-KO mice, suggesting that disruption of p53 activates YAP. These findings are in accordance with a recent report showing that the loss of p53 activates YAP in KRAS-driven mouse pancreatic adenocarcinoma,³⁸ in which a YAP-*Myc*-*Sox2*-p53 regulatory network has been implicated to be critical in metabolic homeostasis and differentiation of the tumors.³⁹ Interestingly, YAP has also been reported to be involved in the regulation of stem cell differentiation.^{40,41} Our study highlights a close mutual relationship among *Myc*, YAP, and p53 in the regulation of differentiation of hepatocyte-derived tumors.

The expression levels of AFP and DLK1 in the HRAS/*Myc*-induced tumors were higher in the homozygous p53-KO mice than in the heterozygous p53-KO mice, indicating a more dedifferentiated state in the former. This finding is compatible with the less-differentiated histological features of the tumors with inconspicuous ductular structures and with a significant decrease in the mRNA expression of *Hnf4a* and *Sox9*. Interestingly, it has been shown that the phenotype of hepatoblastoma-like tumors induced by *Myc* can be modified to that of cHCC-CCA through the suppression of the NF- κ B signaling pathway.⁴² Blocking the NF- κ B signaling pathway has been reported to facilitate the differentiation of HCC, which is mediated by a variant of the histone H2A, MacroH2A1.⁴³ Taken together, the findings show that, although dedifferentiation of the transformed hepatocytes can generate tumors with a bipotential phenotype, dedifferentiation exceeding certain threshold levels leads to the expression of more hepatoblastic features and therefore may abolish either hepatocytic or biliary differentiation.

The phosphorylation levels of ERK were decreased in the HRAS/*Myc*-induced tumors in the p53-KO mice, especially in the homozygous p53-KO mice, which showed more marked dedifferentiation. Because the introduction of *Myc* alone is insufficient to induce liver tumor formation in our system, the activation of the RAS pathway is indispensable for the hepatocarcinogenesis in HRAS/*Myc*-induced tumors.^{15,18} However, our results suggest that the acquisition of the dedifferentiated phenotype is closely associated with the suppression of ERK function. The inhibition of *Sox9* mRNA expression in the HRAS/*Myc*-induced tumors with p53 disruption might be explained by the decreased ERK phosphorylation, as *Sox9* has been shown to be a downstream effector of the EGFR signaling mediated by ERK.⁴⁴ It has been demonstrated that the maintenance of murine pluripotent stem cells requires the suppression of ERK signaling through the activation of dual-specificity phosphatases that are transcriptionally

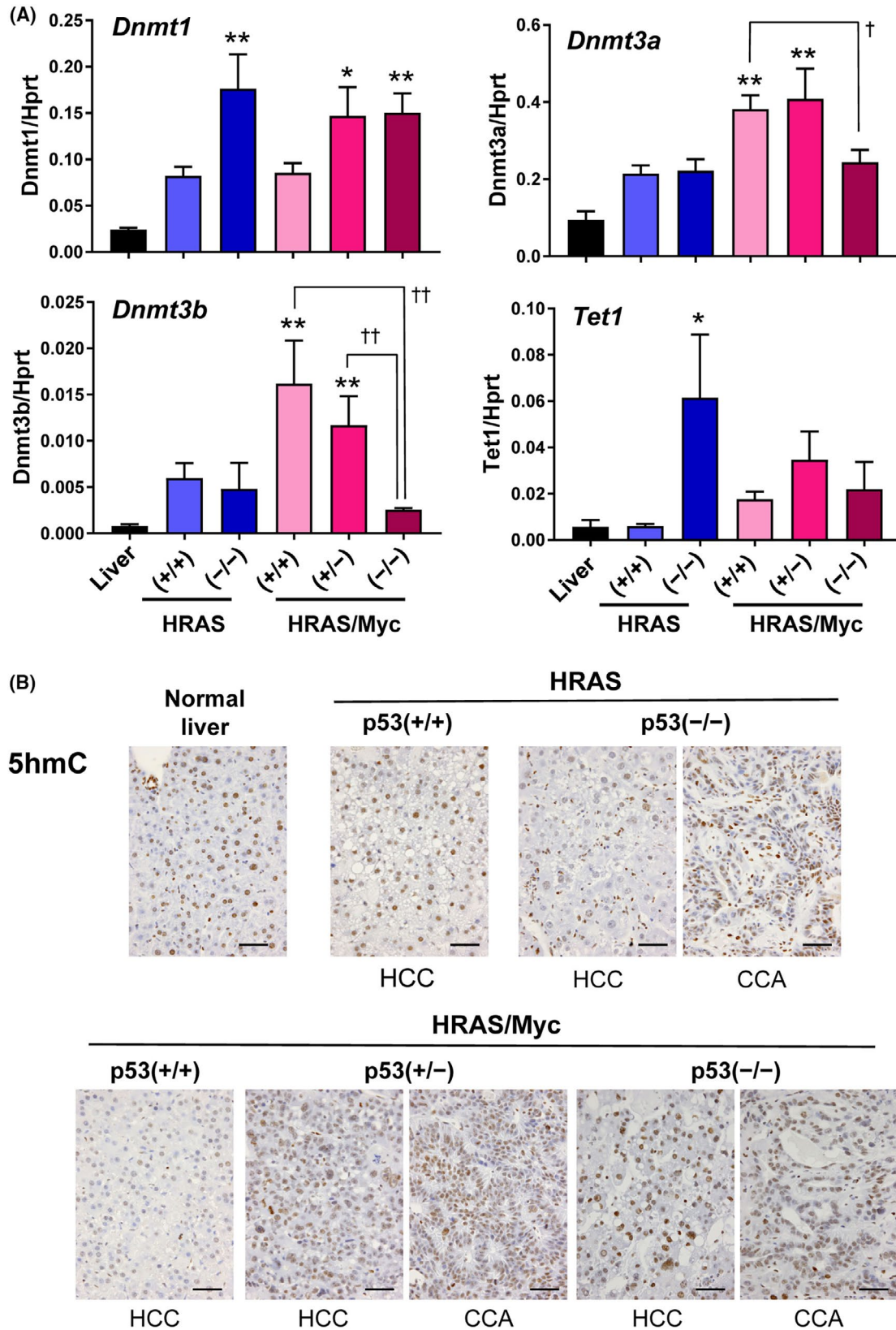


FIGURE 5 Effects of p53 disruption on the mRNA expression of the genes coding proteins involved in DNA methylation and demethylation in tumors induced by HRAS or HRAS/Myc. A, Quantitative RT-PCR analyses of the mRNA expression of DNA methyltransferases (*Dnmt1*, *Dnmt3a*, and *Dnmt3b*) and a DNA demethylase (*Tet1*). p53(+/+), wild type; p53(+/-), heterozygous p53-KO; and p53(-/-), homozygous p53-KO. n = 4 for normal liver, HRAS (+/+), and HRAS (-/-); n = 6 for HRAS/Myc (+/+), HRAS/Myc (+/-), and HRAS/Myc (-/-). Statistical analyses: Kruskal-Wallis test, **P* < .05 and ***P* < .01 (vs normal liver); Mann-Whitney *U* test, †*P* < .05 and ††*P* < .01. B, Immunohistochemistry for 5hmC. p53(+/+), wild type; p53(+/-), heterozygous p53-KO; and p53(-/-), homozygous p53-KO. Scale bar = 40 μm

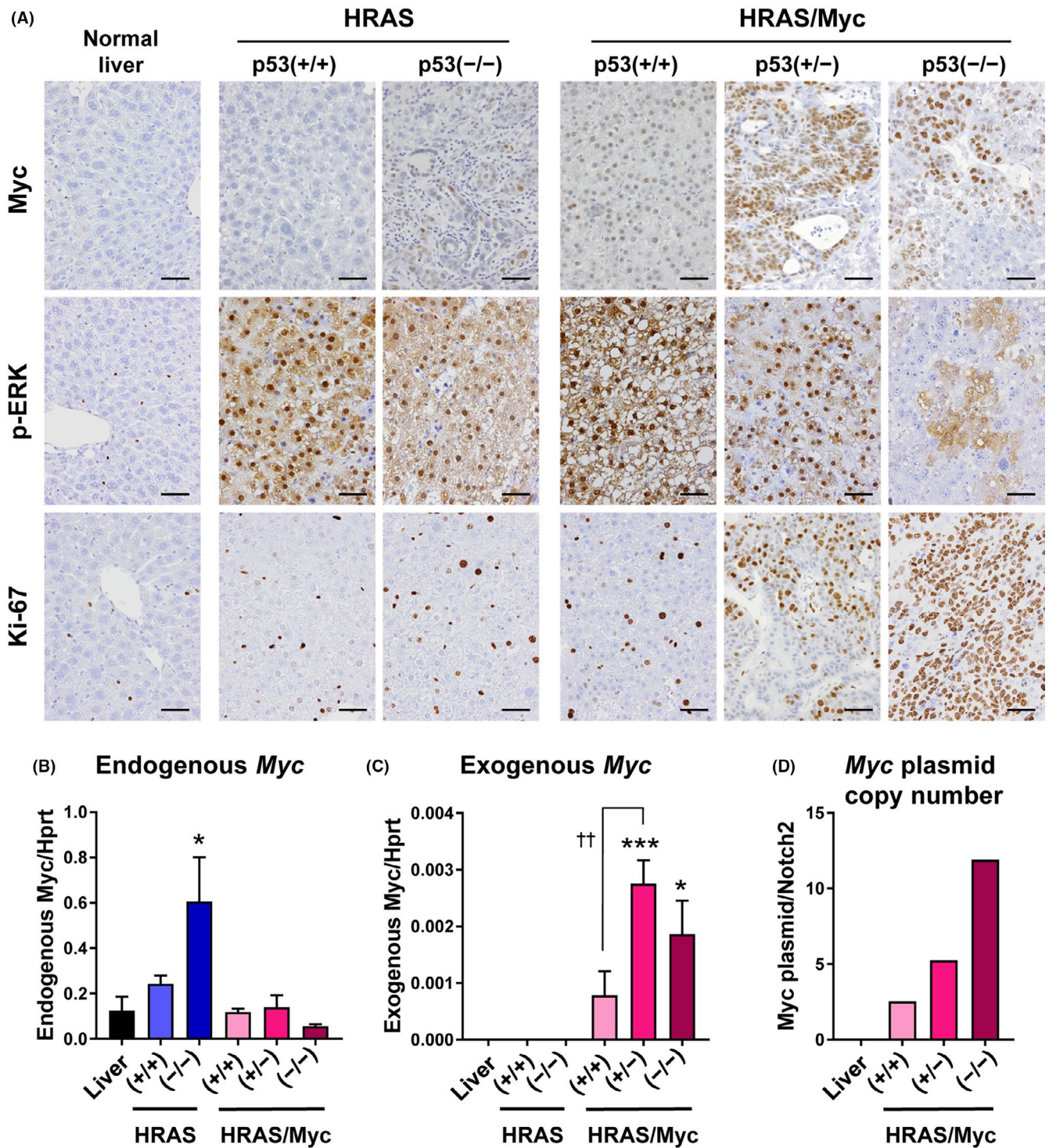


FIGURE 6 Effects of p53 disruption on the expression of Myc, the phosphorylation of ERK, and a proliferation marker and the mRNA expression of Myc in tumors induced by HRAS or HRAS/Myc. A, Immunohistochemistry for Myc, phosphorylated ERK, and Ki-67. p53(+/+), wild type; p53(+/-), heterozygous p53-KO; and p53(-/-), homozygous p53-KO. Scale bar = 40 μ m. B, C, Quantitative RT-PCR analyses of the mRNA expression of endogenous Myc (B) and exogenous Myc (C). p53(+/+), wild type; p53(+/-), heterozygous p53-KO; and p53(-/-), homozygous p53-KO. n = 4 for normal liver, HRAS (+/+), and HRAS (-/-); n = 6 for HRAS/Myc (+/+), HRAS/Myc (+/-), and HRAS/Myc (-/-). Statistical analyses: one-way analysis of variance (ANOVA) with Tukey's post hoc test, * P < .05, *** P < .001 (vs normal liver); unpaired two-tailed t -test, †† P < .01. D, Estimation of the copy number of the integrated Myc plasmid in HRAS/Myc-induced liver tumors. The amounts of genomic DNA from tumor samples were normalized by the estimation of the copy numbers of the endogenous Notch2 gene. The data are presented as the means of two independent experiments (n = 3 each) that showed similar results

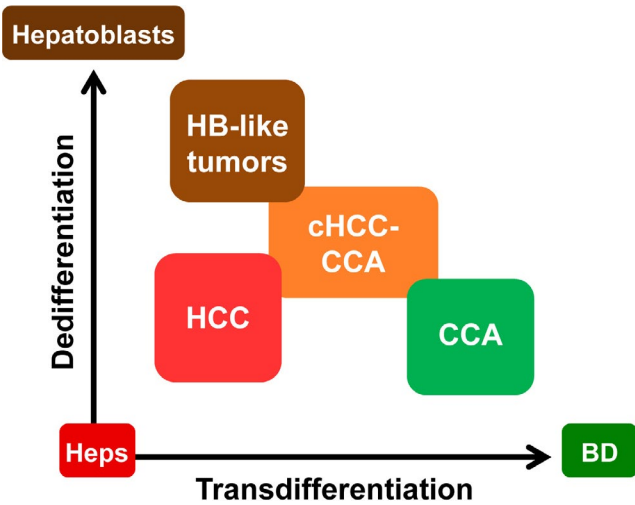


FIGURE 7 Schematic diagram of the interrelationships among various phenotypes of liver tumors originating from hepatocytes. Two-dimensional perspective of the hepatocyte-derived tumors with respect to transdifferentiation and dedifferentiation. HB, hepatoblastoma; HCC, hepatocellular carcinoma; CCA, intrahepatic cholangiocarcinoma; Heps, hepatocytes; BD, bile ducts/ductules

activated by Myc/Max complexes.⁴⁵ Furthermore, the suppression of ERK by Myc activation has been shown to be required for somatic cell reprogramming.⁴⁶ Our findings indicate that mature hepatocytes can acquire a stem cell-like reprogrammed phenotype, which is compatible with a previous report.⁴⁷

Liver tumors induced by HRAS or HRAS/Myc have been shown to be associated with changes in the mRNA expression of enzymes involved in DNA methylation and demethylation.²⁰ In the present study, p53 KO was found to increase the mRNA expression of a maintenance DNA methyltransferase (*Dnmt1*) in both the HRAS-induced and HRAS/Myc-induced tumors, whereas homozygous p53 KO suppressed the increase in the mRNA expression of de novo DNA methyltransferases (*Dnmt3a* and *Dnmt3b*) in the HRAS/Myc-induced tumors. In addition, the mRNA expression of a DNA demethylase (*Tet1*) in the HRAS-induced tumors was enhanced by p53 KO. p53 KO has been shown to induce the mRNA expression of *Dnmt1*, *Dnmt3a*, and *Dnmt3b* in the livers of p53-KO mice.⁴⁸ Our results of 5hmC immunohistochemistry suggests that active demethylation takes place in the tumors with p53 disruption. Although comprehensive studies regarding the DNA methylation status are needed to fathom the significance of these findings, our results suggest that p53 plays significant roles in epigenetic regulation of primary liver cancers.

We previously reported that the cointroduction of HRAS and Myc by the original transposon cassette vectors in wild-type mice induced dedifferentiated liver tumors with high levels of AFP, IGF2, and DLK1 expression but without ductular transdifferentiation or CK19 expression (Supplementary Figure 2A).²⁰ Foci of extramedullary hematopoiesis were occasionally found within the tumors, suggesting the acquisition of hepatoblastic features (Supplementary Figure 2B). These dedifferentiated tumors expressed Myc at high levels and were highly proliferative, but ERK phosphorylation was

markedly suppressed (Supplementary Figure 2C). Although the phenotype of the HRAS/Myc-induced tumors was different in the present study, with transposon cassette vectors modified by the deletion of two loxP sites, dedifferentiated features were evident when p53 was disrupted. The emergence of the dedifferentiated phenotype was closely associated with the increased expression of the Myc protein and the suppression of ERK phosphorylation, as in the tumors induced by the original plasmids. The number of integrated copies of the Myc plasmid was 10.2-fold greater and the level of Myc mRNA expression was 17.8 times higher in the liver tumors induced by the original HRAS and Myc plasmids in the wild-type mice than in those induced by the modified plasmids in the wild-type mice (data not shown). Although the reason for the inefficient integration and low level of Myc expression in the modified Myc plasmid is not currently clear, our results demonstrate that Myc expression and the suppression of ERK phosphorylation are closely correlated with the dedifferentiated phenotype of hepatocyte-derived tumors and that the loss of p53 enhances the dedifferentiation at least partly through the enhanced expression of Myc protein.

In conclusion, our study demonstrates that the loss of p53 confers hepatocyte-derived liver cancers with biliary differentiation through transdifferentiation or dedifferentiation and that the latter can be mediated by Myc activation. From our experimental data, we propose a two-dimensional perspective on the understanding of a wide spectrum of hepatocytic tumors: In extreme cases, transformed hepatocytes can generate CCA through transdifferentiation, whereas they can generate hepatoblastoma-like tumors without definitive hepatocytic or biliary features through dedifferentiation; cHCC-CCA might be tumors generated through partial transdifferentiation or dedifferentiation (Figure 7).

ACKNOWLEDGMENTS

We thank Mr Yoshiyasu Satake for animal care and Ms Aya Kitano for administrative assistance.

DISCLOSURE

The authors have no conflicts of interest.

ORCID

Yusuke Mizukami  <https://orcid.org/0000-0002-1068-7024>

Yuji Nishikawa  <https://orcid.org/0000-0002-4774-1936>

REFERENCES

1. Brunt E, Aishima S, Clavien PA, et al. cHCC-CCA: Consensus terminology for primary liver carcinomas with both hepatocytic and cholangiocytic differentiation. *Hepatology*. 2018;68:113-126.
2. Tickoo SK, Zee SY, Obiekwe S, et al. Combined hepatocellular-cholangiocarcinoma: a histopathologic, immunohistochemical, and in situ hybridization study. *Am J Surg Pathol*. 2002;26:989-997.
3. Miyajima A, Tanaka M, Itoh T. Stem/progenitor cells in liver development, homeostasis, regeneration, and reprogramming. *Cell Stem Cell*. 2014;14:561-574.
4. Kopp JL, Grompe M, Sander M. Stem cells versus plasticity in liver and pancreas regeneration. *Nat Cell Biol*. 2016;18:238-245.

5. Shiojiri N, Katayama H. Secondary joining of the bile ducts during the hepatogenesis of the mouse embryo. *Anat Embryol (Berl)*. 1987;177:153-163.
6. Nagahama Y, Sone M, Chen X, et al. Contributions of hepatocytes and bile ductular cells in ductular reactions and remodeling of the biliary system after chronic liver injury. *Am J Pathol*. 2014;184:3001-3012.
7. McCright B, Lozier J, Gridley T. A mouse model of Alagille syndrome: Notch2 as a genetic modifier of Jag1 haploinsufficiency. *Development*. 2002;129:1075-1082.
8. Duncan AW, Dorrell C, Grompe M. Stem cells and liver regeneration. *Gastroenterology*. 2009;137:466-481.
9. Michalopoulos GK, Barua L, Bowen WC. Transdifferentiation of rat hepatocytes into biliary cells after bile duct ligation and toxic biliary injury. *Hepatology*. 2005;41:535-544.
10. Nishikawa Y, Doi Y, Watanabe H, et al. Transdifferentiation of mature rat hepatocytes into bile duct-like cells in vitro. *Am J Pathol*. 2005;166(4):1077-1088.
11. Yanger K, Zong Y, Maggs LR, et al. Robust cellular reprogramming occurs spontaneously during liver regeneration. *Genes Dev*. 2013;27:719-724.
12. Carlson CM, Frandsen JL, Kirchhof N, Mclvor RS, Largaespada DA. Somatic integration of an oncogene-harboring Sleeping Beauty transposon models liver tumor development in the mouse. *Proc Natl Acad Sci U S A*. 2005;102:17059-17064.
13. Chen X, Calvisi DF. Hydrodynamic transfection for generation of novel mouse models for liver cancer research. *Am J Pathol*. 2014;184:912-923.
14. Ho C, Wang C, Mattu S, et al. AKT (v-akt murine thymoma viral oncogene homolog 1) and N-Ras (neuroblastoma ras viral oncogene homolog) coactivation in the mouse liver promotes rapid carcinogenesis by way of mTOR (mammalian target of rapamycin complex 1), FOXM1 (forkhead box M1)/SKP2, and c-Myc pathways. *Hepatology*. 2012;55:833-845.
15. Xin B, Yamamoto M, Fujii K, et al. Critical role of Myc activation in mouse hepatocarcinogenesis induced by the activation of AKT and RAS pathways. *Oncogene*. 2017;36:5087-5097.
16. Fan B, Malato Y, Calvisi DF, et al. Cholangiocarcinomas can originate from hepatocytes in mice. *J Clin Invest*. 2012;122:2911-2915.
17. Li T, Mo X, Fu L, Xiao B, Guo J. Molecular mechanisms of long non-coding RNAs on gastric cancer. *Oncotarget*. 2016;7:8601-8612.
18. Yamamoto M, Xin B, Watanabe K, et al. Oncogenic determination of a broad spectrum of phenotypes of hepatocyte-derived mouse liver tumors. *Am J Pathol*. 2017;187:2711-2725.
19. Coulouarn C, Cavard C, Rubbia-Brandt L, et al. Combined hepatocellular-cholangiocarcinomas exhibit progenitor features and activation of Wnt and TGFbeta signaling pathways. *Carcinogenesis*. 2012;33:1791-1796.
20. Watanabe K, Yamamoto M, Xin B, et al. Emergence of the dedifferentiated phenotype in hepatocyte-derived tumors in mice: roles of oncogene-induced epigenetic alterations. *Hepatol Commun*. 2019;3:697-715.
21. Anonymous. Comprehensive and integrative genomic characterization of hepatocellular carcinoma. *Cell*. 2017;169:1327-1341 e1323.
22. Moeini A, Sia D, Zhang Z, et al. Mixed hepatocellular cholangiocarcinoma tumors: cholangiolocellular carcinoma is a distinct molecular entity. *J Hepatol*. 2017;66:952-961.
23. Liu ZH, Lian BF, Dong QZ, et al. Whole-exome mutational and transcriptional landscapes of combined hepatocellular cholangiocarcinoma and intrahepatic cholangiocarcinoma reveal molecular diversity. *Biochim Biophys Acta Mol Basis Dis*. 2018;1864:2360-2368.
24. Joseph NM, Tsokos CG, Umetsu SE, et al. Genomic profiling of combined hepatocellular-cholangiocarcinoma reveals similar genetics to hepatocellular carcinoma. *J Pathol*. 2019;248:164-178.
25. Katz SF, Lechel A, Obenauf AC, et al. Disruption of Trp53 in livers of mice induces formation of carcinomas with bilineal differentiation. *Gastroenterology*. 2012;142(5):1229-1239.e3.
26. Dai MS, Jin Y, Gallegos JR, Lu H. Balance of Yin and Yang: ubiquitylation-mediated regulation of p53 and c-Myc. *Neoplasia*. 2006;8:630-644.
27. Totaro A, Castellan M, Di Biagio D, Piccolo S. Crosstalk between YAP/TAZ and Notch Signaling. *Trends Cell Biol*. 2018;28:560-573.
28. Dauch D, Rudalska R, Cossa G, et al. A MYC-aurora kinase A protein complex represents an actionable drug target in p53-altered liver cancer. *Nat Med*. 2016;22:744-753.
29. Li L, Qian M, Chen IH, et al. Acquisition of cholangiocarcinoma traits during advanced hepatocellular carcinoma development in mice. *Am J Pathol*. 2018;188:656-671.
30. Takahashi K, Tanabe K, Ohnuki M, et al. Induction of pluripotent stem cells from adult human fibroblasts by defined factors. *Cell*. 2007;131:861-872.
31. Shachaf CM, Kopelman AM, Arvanitis C, et al. MYC inactivation uncovers pluripotent differentiation and tumour dormancy in hepatocellular cancer. *Nature*. 2004;431:1112-1117.
32. Ho JS, Ma W, Mao DY, Benchimol S. p53-Dependent transcriptional repression of c-myc is required for G1 cell cycle arrest. *Mol Cell Biol*. 2005;25:7423-7431.
33. Porter JR, Fisher BE, Baranello L, et al. Global inhibition with specific activation: how p53 and MYC redistribute the transcriptome in the DNA double-strand break response. *Mol Cell*. 2017;67(6):1013-1025.e9.
34. Sachdeva M, Zhu S, Wu F, et al. p53 represses c-Myc through induction of the tumor suppressor miR-145. *Proc Natl Acad Sci U S A*. 2009;106:3207-3212.
35. Feng YC, Liu XY, Teng L, et al. c-Myc inactivation of p53 through the pan-cancer lncRNA MILIP drives cancer pathogenesis. *Nat Commun*. 2020;11:4980.
36. Zindy F, Eischen CM, Randle DH, et al. Myc signaling via the ARF tumor suppressor regulates p53-dependent apoptosis and immortalization. *Genes Dev*. 1998;12:2424-2433.
37. Akita H, Marquardt JU, Durkin ME, et al. MYC activates stem-like cell potential in hepatocarcinoma by a p53-dependent mechanism. *Cancer Res*. 2014;74:5903-5913.
38. Mello SS, Valente LJ, Raj N, et al. A p53 super-tumor suppressor reveals a tumor suppressive p53-Ptpn14-Yap axis in pancreatic cancer. *Cancer Cell*. 2017;32(4):460-473.e6.
39. Murakami S, Nemazany I, White SM, et al. A Yap-Myc-Sox2-p53 regulatory network dictates metabolic homeostasis and differentiation in Kras-driven pancreatic ductal adenocarcinomas. *Dev Cell*. 2019;51(1):113-128.e9.
40. Lian I, Kim J, Okazawa H, et al. The role of YAP transcription coactivator in regulating stem cell self-renewal and differentiation. *Genes Dev*. 2010;24:1106-1118.
41. Passaro F, De Martino I, Zambelli F, et al. YAP contributes to DNA methylation remodeling upon mouse embryonic stem cell differentiation. *J Biol Chem*. 2021;296:100138.
42. He J, Gerstenlauer M, Chan LK, et al. Block of NF-kB signaling accelerates MYC-driven hepatocellular carcinogenesis and modifies the tumor phenotype towards combined hepatocellular cholangiocarcinoma. *Cancer Lett*. 2019;458:113-122.
43. Lo Re O, Fusilli C, Rappa F, et al. Induction of cancer cell stemness by depletion of macrohistone H2A1 in hepatocellular carcinoma. *Hepatology*. 2018;67:636-650.
44. So J, Kim M, Lee SH, et al. Attenuating the epidermal growth factor receptor-extracellular signal-regulated kinase-sex-determining region Y-Box 9 axis promotes liver progenitor cell-mediated liver regeneration in zebrafish. *Hepatology*. 2021;73:1494-1508.

45. Chappell J, Sun Y, Singh A, Dalton S. MYC/MAX control ERK signaling and pluripotency by regulation of dual-specificity phosphatases 2 and 7. *Genes Dev.* 2013;27:725-733.
46. Huh S, Song HR, Jeong GR, et al. Suppression of the ERK-SRF axis facilitates somatic cell reprogramming. *Exp Mol Med.* 2018;50:e448.
47. Holczbauer A, Factor VM, Andersen JB, et al. Modeling pathogenesis of primary liver cancer in lineage-specific mouse cell types. *Gastroenterology.* 2013;145:221-231.
48. Park IY, Sohn BH, Choo JH, et al. Deregulation of DNA methyltransferases and loss of parental methylation at the insulin-like growth factor II (Igf2)/H19 loci in p53 knockout mice prior to tumor development. *J Cell Biochem.* 2005;94:585-596.

SUPPORTING INFORMATION

Additional supporting information may be found online in the Supporting Information section.

How to cite this article: Liu Y, Xin B, Yamamoto M, et al. Generation of combined hepatocellular-cholangiocarcinoma through transdifferentiation and dedifferentiation in p53-knockout mice. *Cancer Sci.* 2021;112:3111–3124. <https://doi.org/10.1111/cas.14996>